AIAA-91-0285

Primary Breakup in Liquid/Gas Mixing Layers

P.-K. Wu, G. A. Ruff and G. M. Faeth
Department of Aerospace Engineering
The University of Michigan, Ann Arbor, Michigan

29th Aerospace Sciences Meeting
January 7–10, 1991/Reno, Nevada

AIAA-91-0285

Primary Breakup in Liquid/Gas Mixing Layers

P.-K. Wu, G. A. Ruff and G. M. Faeth
Department of Aerospace Engineering
The University of Michigan, Ann Arbor, Michigan

Abstract

An experimental study of primary breakup in the near-injector region of large diameter (5.0 and 9.5 mm) liquid jets in still air is described. Measurements involved flash photography and holography to provide flow visualization and drop size distributions for initially nonturbulent liquids (water, n-heptane and various glycerol mixtures) having various jet exit velocities. Drop sizes after primary breakup satisfied Simmons' universal root normal distribution and can be characterized solely by their SMD. The SMD increased with distance from the jet exit and then remained nearly constant within a fully-developed primary breakup region. SMD measurements in the fully-developed regime did not agree with existing expressions based on unstable surface wave growth. However, an expression based on stripping-type breakup due to boundary layer growth in the liquid along the windward side of surface waves yielded a reasonably good correlation of present SMD measurements. The nature of this primary breakup correlation implies that secondary breakup is a dominant feature of liquid/gas mixing layers.

Nomenclature

C_B, C_B', C_B''	= constants in primary breakup correlation
d	= jet exit diameter
d_{max}, d_{min}	= maximum and minimum image dimensions of drops
d_p	= drop diameter
e_p	= drop ellipticity
MMD	= mass median diameter
Oh	= jet exit Ohnesorge number, $\mu_f/(\rho_f d\sigma)^{1/2}$
Re_{fd}	= jet exit Reynolds number, $\rho_f d\bar{u}_o/\mu_f$
Re_{fx}	= Reynolds number based on distance from the jet exit, $\rho_f x\bar{u}_o/\mu_f$
SMD	= Sauter mean diameter
Ta	= Taylor number, $(\rho_g/\rho_f)^{1/2}\mu_f\bar{u}_o/\sigma$
$\bar{u}_o$	= mean jet exit velocity
We_{gd}	= jet exit Weber number, $\rho_g d\bar{u}_o^2/\sigma$
We_{gp}	= drop Weber number, $\rho_g d_p\bar{u}_o^2/\sigma$
We_{gSMD}	= spray Weber number, $\rho_g SMD\bar{u}_o^2/\sigma$
x	= distance from jet exit
Δp	= stagnation pressure rise of liquid
μ	= molecular viscosity
ρ	= density
σ	= surface tension
Subscripts	
f	= liquid-phase property
FD	= property in fully-developed primary breakup regime
g	= gas-phase property

* Graduate Assistant, Department of Aerospace Engineering.
† Graduate Assistant, Department of Aerospace Engineering; currently, Assistant Professor, Department of Mechanical Engineering, Drexel University, Philadelphia, Pennsylvania.
‡Professor, Department of Aerospace Engineering, Fellow, AIAA.

Introduction

An experimental investigation of dispersed liquid generation along liquid surfaces within liquid/gas mixing layers (primary breakup) is described. The study was motivated by the importance of primary breakup within the near-injector region of pressure-atomized sprays as well as for gas jets in liquids. Drop size distributions after primary breakup were measured within multiphase mixing layers formed about the periphery of round liquid jets in still room air. Various liquids and relative velocities were considered for low turbulence intensity slug flows at the jet exit. The measurements were used to evaluate existing and proposed theories and correlations of mean drop sizes after primary breakup. The objective was to extend recent work concerning the structure and mixing properties of the dense-spray region of pressure-atomized sprays,[1-4] to focus on primary breakup, since this process has a major influence on the rate of development, and the importance of separated flow effects, for these flows.

A number of reviews of liquid atomization and dense sprays have appeared;[2-11] therefore, only the main features of past work will be considered. The discussion also will be limited to the wind-induced and atomization breakup regimes, defined by Miesse[12] and Ranz,[13] since they are most important for practical applications, e.g., the other breakup regimes are limited to a small range of low jet velocities and yield large drops that are not very effective for dispersing and mixing the liquid. Within these regimes, primary breakup occurs along the liquid surface within a multiphase mixing layer adjacent to the surface. Both theories and measurements of primary breakup properties in this flow will be considered in the following.

Past theories seeking to provide correlations of drop sizes after primary breakup have mainly been limited to mean drop sizes for nonturbulent liquids. Two major approaches have been proposed: (1) aerodynamic breakup based on linear wave growth theory which was initially proposed by Taylor,[14] with subsequent development by Ranz[13] and Levich,[15] and later application by Reitz and Bracco,[16] among others; and (2) sheltered wave growth theory due to Mayer[17] and Adelberg[18] which rests on the surface wave growth model of Jeffreys.[19] Taylor's[14] aerodynamic breakup model involves assuming proportionality between the most rapidly growing waves on the liquid surface and the mean drop size (taken to be the Sauter mean diameter, SMD, in the following) after primary breakup. Wave growth properties are found from linear stability theory allowing for effects of aerodynamic forces due to gas flowing across the waves as well as the stabilizing effects of surface tension and liquid viscosity. This yields a relatively complex relationship between the Weber number based on SMD after primary breakup, $We_{gSMD} = \rho_g SMD\bar{u}_o^2/\sigma$, and what will be termed the Taylor number, $Ta = (\rho_g/\rho_f)^{1/2}\mu_f\bar{u}_o/\sigma$. This form implies that the mean jet exit velocity, $\bar{u}_o$, is the proper relative velocity near the surface, which is justified by the measurements of Ruff et al.[2,3] for multiphase mixing layers near the jet exit. Ranz[13] and Levich[15] propose simpler limiting behavior at small Ta, where effects of liquid viscosity can be neglected, yielding:

$$We_{gSMD} = C_B \qquad (1)$$

where C_B is a constant on the order of unity. Levich[15] also undertakes an approximate treatment of effects of liquid viscosity which suggests that We_{gSMD} should increase with

increasing Ta, with primary breakup ceasing when Ta ≈ 1. Experimental confirmation of Eq. (1) and its large Ta behavior, however, has not been reported.

Mayer[17] developed an alternative primary breakup correlation that was also based on wave growth properties. However, he adopted the sheltered wave growth theory of Jeffreys[19] to find wave properties, since this approach had achieved some success in predicting the properties of wind-induced ripples on wave surfaces. This yields

$$We_{gSMD} = C_B'Ta^{2/3} \qquad (2)$$

where Mayer[17] recommends $C_B' = 21$ based on measurements of Weiss and Worsham.[20] This expression was adopted for the JANNAF liquid rocket performance code although it became evident that C_B' had to be varied over an order of magnitude to achieve reasonable predictions for various injector systems.[7] Adelberg[18] developed a primary breakup expression along the same lines as Mayer[17] but suggests $C_B' = 45$, which represents one of many subsequent variations C_B' to match limited ranges of particular data sets, as noted earlier. In particular, it is probable that the data used to fit Eq. (2) by both Mayer[17] and Adelberg[18] was influenced by secondary breakup, since the measurements were made far from the injector within the dilute portions of sprays.

In contrast to the theories,[14-18] which do not consider effects of liquid vorticity, most measurements of the near injector properties of dense sprays have exhibited strong effects of liquid flow properties at the jet exit.[1-4,8,21-24] In particular, Phinney[21] finds that transition between the wind-induced and atomization breakup regimes is affected by the presence of liquid turbulence at the jet exit.[8] The degree of flow development at the jet exit was also found to influence initial mixing rates of liquid jets in gases, with fully-developed turbulent pipe flow yielding much faster mixing rates than nonturbulent slug flows.[1,4] This must involve effects of liquid turbulence on primary breakup, since this process controls the initial dispersion of liquid. Additionally, visualization of the flow by Hoyt and Taylor[22-24] indicated very little effect of relative velocities on the initial breakup for a fixed jet exit velocity, completely contradicting properties anticipated from the primary breakup theories. This implies that liquid vorticity within boundary layers developing in the nozzle passage dominates primary breakup very near the jet exit, which is plausible because of the importance of liquid vorticity due to the large density ratio of liquid/gas mixing layers. Finally, measurements of drop size distributions after primary breakup for water jets in room air, at a single relative velocity, showed a much larger SMD for turbulent pipe flow than for nonturbulent slug flow.[3] Thus, experiments exhibit a variety of features that are not anticipated by existing models of primary breakup, however, the existing measurements are far too limited, water in room air at a single relative velocity,[3] to provide an adequate evaluation of predictions and needed direction for new development of theory.

The successful development of holography techniques to provide observations of primary breakup properties within liquid/gas mixing layers provides a means of addressing this gap in the literature.[2,3] Thus, the objective of the present investigation was to observe primary breakup using pulsed holography, to exploit the results to evaluate existing theories,[14-18] and to develop alternatives where necessary. The experiments involved relatively large diameter nonevaporating liquid jets (5.0 and 9.5 mm) injected into still room air with nonturbulent slug flow at the jet exit. This provided a relatively long multiphase mixing layer so that jet exit disturbances could decay to reveal the fundamental evolution of primary breakup properties with position within the mixing layer. Various liquids (water, n-heptane and glycerol solutions) and jet exit velocities were considered in order to examine the effect of a wide range of liquid damping and aerodynamic properties.

The paper begins with a brief description of experimental methods. Results are then described considering flow visualization and primary breakup properties in turn.

Experimental Methods

Apparatus

The objective of the measurements was to resolve effects of liquid properties and relative velocities on primary breakup within multiphase mixing layers. Additionally, good optical access was a prime consideration. Thus, the test flows involved injection of modest amounts of liquid, to control costs, into still air at room conditions, to avoid optical distortion due to windows. The arrangement also accommodated large injector pressure drops (up to 35 MPa) so that a wide range of relative velocities across the mixing layer (up to 300 m/s) could be examined.

Figure 1 is a sketch of the injector system. The test liquid is placed within an accumulator having the jet nozzle passage at the bottom. Premature liquid outflow is prevented by placing a cork in the nozzle exit. The liquid is then forced through the nozzle, ejecting the cork at the start of the flow, by admitting high pressure air to the top of the accumulator through a solenoid actuated valve. A piston within the accumulator, sealed along its sides, prevents mixing between the air and the test liquid. The piston is hydraulically cushioned at the end of its travel in order to reduce shock and vibration of the apparatus. After venting air from the top of the piston, it is returned to the top of the accumulator so that the system can be refilled with liquid. The cork closure in the nozzle exit allowed the liquid to be filled from the bottom of the accumulator while venting trapped air from just below the piston face.

The high pressure air is supplied from a pressure intensifier that also serves as the air storage system for the accumulator. The laboratory air supply system can be used to charge the accumulator and no pressure intensification is needed for injection pressures up to 17 MPa. For higher pressure drops, air is first vented into the pressure intensifier to the maximum supply pressure with only a small quantity of oil in the bottom. Oil is then pumped into the bottom of the intensifier, reducing the gas volume and increasing the gas pressure to the desired level. The system is then sealed prior to execution of a test. At the end of operation, the oil is vented from the pressure intensifier and the filling process is repeated for the next test.

The piston has a diameter of 64 mm and a stroke of 200 mm, yielding a liquid sample size of roughly 600 mℓ. Testing was limited to 5.0 mm diameter slug flow at the jet exit. The contraction section of the nozzle was designed according to Smith and Wang[25] to provide a uniform velocity across the exit, aside from boundary layers along the walls of the passage. Detailed measurements of jet exit properties have not been made but turbulence levels are expected to be low due to the relatively quiescent conditions at the start of contraction and the large nozzle contraction ratio (roughly 100:1).[26] Injection is vertically downward with the liquid captured in a baffled tub and then discarded. Instrumentation is mounted rigidly; therefore, various positions in the flow are studied by moving the injector with positioning accuracies of 5 μm in the horizontal direction and 0.5 mm in the vertical direction.

Total times of injection were 230-1140 ms. These relatively short time periods were not problematical, however,

because flow development times are short for the near-injector region of the mixing layer, roughly 4-30 ms. Additionally, measurements are made using flash photography and pulsed holography which require times less than 1-2 μs for data accumulation.

Instrumentation

Pressure Measurements. Apparatus performance was monitored by pressure measurements at the inlet of the accumulator using a piezoelectric transducer (Kistler Corp., Model 211B2) whose output was recorded with a digital oscilloscope (LeCroy, Model 9400A).

Injector performance for a given liquid and accumulator pressure was tested using an impact plate. This involved a rectangular plate (125 × 175 mm) whose center coincided with the injector axis, located 25 mm from the jet exit. A piezoelectric pressure transducer and oscilloscope, identical to the arrangement used to measure the accumulator pressure, were used to measure the impact pressure at the center of the plate. The measured stagnation pressure difference then yielded the mean jet exit velocity as follows: $\bar{u}_o = (2\Delta p/\rho_f)^{1/2}$.

Flash Photography. Flash photography was used to observe the overall appearance of the flows. The photographs were obtained in a darkened room with an open camera shutter, with the exposure time limited by the flash duration. The light source was a Xenon Corp. high intensity micropulse system (Model 457A), which can provide up to a 10 J light pulse with a duration of roughly 1 μs. A 4 × 5 Speed Graphic camera was used to record the image, loaded with Polaroid type 57 black-and-white film (ASA 3000). The sprays were photographed in 100 mm long sections in order to provide reasonable spatial resolution.

Holography. A single-pulse holography system, similar to earlier work,[2,3] was used to measure drop size distributions. An off-axis arrangement was used, based on the Spectron Development Laboratories Model HTRC-5000 system, with an angle of 28° between the object and reference beams. Adequate spatial resolution and sufficient light intensity to penetrate the spray was provided by reducing the diameter of the object beam through the spray and then expanding it (7-8:1) back to the same diameter (85 mm) as the reference beam when the two signals were optically mixed to form the hologram. The holograms were generated by a ruby laser that deposited 50 mJ in roughly 20 ns. This effectively stopped the flow so that objects as small as 5 μm in diameter could be measured. The holograms were obtained in a darkened room using AGFA 8E75HD-NAH unbacked holographic film plates having a 100 × 125 mm format.

The holograms were reconstructed using a 15 mW HeNe laser beam that was expanded to a diameter of 50 mm to provide a real image of the spray in front of the hologram. The properties of the reconstructed spray were observed with an MTI Model 65 video camera with optics to provide a field of view of 1.4 × 1.6 mm. Computer controlled x-y traversing of the hologram (1 μm resolution) and z traversing of the video camera (5 μm resolution) allowed observation of the entire object field. The video image was analyzed using a Gould FD5000 image processing system. Reference pins of known size and location near the edge of the object field provided direct calibration of distances on the reconstructions.

Drops and other ellipsoidal objects were sized by measuring their maximum and minimum diameters through the centroid of the image. Assuming ellipsoidal shapes, the diameter of these objects was taken to be the diameter of an ellipsoid having the same volume, i.e., $d_p^3 = d_{min}^2 d_{max}$. The shape of the object was also characterized by its ellipticity, defined as $e_p = d_{max}/d_{min}$. This approach was not feasible, however, for irregular liquid elements or in cases where the centroid was not located within the boundaries of the image. Then, the crossectional area and perimeter of the image were measured and the maximum and minimum diameters of an ellipsoid having the same crossectional area and perimeter were computed. Given these parameters, the effective diameter and ellipticity were found in the same manner as for drops. The results at each condition were summed, considering 20-400 elements, to provide drop size distributions, mass median diameter (MMD), Sauter mean diameter (SMD) and the volume-averaged ellipticity, e_p.

Experimental uncertainties were generally dominated by finite sampling limitations, since there are relatively few large drops after primary breakup, rather than resolution of liquid element properties from reconstructed holograms. Within the limitations of the definitions of liquid element sizes and ellipticities, which are difficult to quantify, estimates of experimental uncertainties (95 percent confidence) are less than 15 percent for MMD, SMD and volume averaged ellipticity. Uncertainties of drop size distributions are best considered in the context of particular size distribution functions; therefore, these uncertainties will be taken up later.

Test Conditions

Test conditions are summarized in Table 1. A series of holograms for the region along the liquid surface were available from Ruff et al.;[2,3] and were used to provide results for an injector diameter of 9.5 mm. The remainder of the measurements were obtained with the present apparatus that had a jet exit diameter of 5.0 mm. Both injectors involved nonturbulent slug flow at the jet exit.

Test liquids included water, n-heptane, and various glycerin/water mixtures (21, 42 and 63 percent glycerin, by mass). This provided the following ranges of fluid properties: liquid/gas density ratios of 575-975, liquid viscosities of 3.97-108.3 × 10^{-4} kg/ms, and surface tensions of 2.00-7.08 × 10^{-2} N/m. These fluid properties were verified by measuring liquid densities using a hydrometer (Fisher model 11-582, 0.1 percent accuracy), liquid viscosities with a Cannon/Fenske viscometer (Thomas model 9721, 3 percent accuracy) and surface tensions with a ring tensiometer (Fisher model 20, 1 percent accuracy).

Jet exit velocities were in the range 16.5-133.8 m/s, which was sufficient to resolve relative velocity effects without significant uncertainties due to temperature variations from compressibility effects. This yielded ranges of jet dynamic parameters as follows: Re_{fd} of 17,000-750,000, We_{gd} of 94-1520 and Oh of 0.00109-0.0181. All test conditions involved $We_{fd} >> 8$ and $We_{gd} > 40.3$, so that they were well into the atomization breakup regime defined by Miesse[12] and Ranz.[13] According to this classification, the multiphase mixing layer should begin right at the jet exit, however, transition to atomization breakup was also affected by the state of flow development at the jet exit, similar to earlier observations.[1] Thus, some test conditions were in the wind-induced breakup regime, as noted later, where breakup occurs in a multiphase mixing layer that begins at some distance from the jet exit. This deferred transition to atomization breakup was caused by the relatively low levels of flow development and turbulence at the jet exit due to the present slug flow injector design.

Results and Discussion

Flow Visualization

Flash Photography. There were significant differences in the appearance of the flow due to variations of jet exit velocities and liquid viscosities. The latter effect could be broken down into two classes: low viscosity liquids like water and n-heptane, and high viscosity liquids like the glycerol mixtures. Figures 2 and 3 are representative flash photographs near the jet exit for the low (water) and high(63 percent glycerol) viscosity liquids. The region extending up to 65 mm from the jet exit is illustrated for progressively increasing velocities. All these conditions are representative of the atomization breakup regime.

The photographs for the low viscosity liquid (Fig. 2) exhibit progressively increasing flow widths with increasing distance from the jet exit and with jet exit velocity. Growth with respect to distance from the jet exit is expected as the phases continue to mix and drops in the multiphase mixing layer have more time to disperse into the ambient gas. However, the rate of dispersion is somewhat more rapid near the jet exit than farther downstream. Coupled with evidence to be discussed later, this is felt to be due to vorticity generated in the boundary layer along the walls of the injector passage. In particular, the passage is much more effective for retarding the flow at the periphery of the jet than the gas. Thus, it is not unexpected that flow properties near the jet exit differ from positions farther downstream after the initial vortical liquid has undergone primary breakup. Trends with respect to velocity would not be anticipated for single phase jets at these Reynolds numbers, where jets exhibit similarity as a function of r/x, see Ref. 10 and references cited therein. However, this behavior is not unexpected in multiphase jets due to effects of separated flow. In particular, larger relative velocities should yield smaller drop sizes after both primary and secondary breakup with the resulting smaller drops dispersing more rapidly in the radial direction due to reduced effects of separated flow.[10,11] The less mottled appearance of the flow at higher relative velocities seen in Fig. 2 suggests the presence of larger numbers of smaller drops, at least in the visible region near the flow edge, in accord with these expectations.

Results for the high viscosity liquids (Fig. 3) are similar to the low viscosity liquids with respect to general trends with increasing distance from the jet exit and relative velocities. However, in this case differences in behavior from points near the jet exit to points farther downstream are more evident. In particular, streamers of liquid penetrate unusually far into the surroundings yielding almost a bulge in the visible boundary of the jet near the jet exit. This behavior also is consistent with effects of boundary layer growth in the injector passage. In particular, increased liquid viscosity causes increased boundary layer growth in the injector passage with the increased region of vortical liquid providing a greater propensity for breakup of the liquid once the lateral restraint of the passage ends at the jet exit. Additionally, this behavior is consistent with past observations of more rapid mixing of liquid jets in gases as the degree of flow development at the jet exit increases.[1,4,21]

Holography. The hologram reconstructions also exhibit effects of liquid viscosity and streamwise distance on the properties of primary breakup. Typical examples for low (water) and high (glycerol, 63 percent) viscosity liquids are illustrated in Figs. 4 and 5. Results are illustrated at x/d representative of near-injector, transition and conditions approaching the region where effects of initial liquid vorticity are not very significant (ca. x/d = 50). The region pictured is near the liquid surface, which can be seen at the right hand side of each photograph. These photographs were obtained directly from the video monitor of the image analysis system and involve fields of view of roughly 1.5 × 1.5 mm. A difficulty with photographing reconstructions in this manner is that only a few objects are completely in focus due to the limited depth of field of the video camera. In Figs. 4 and 5, the focus has been set to provide a reasonably clear image of the liquid surface and prominent ligaments projecting from the surface.

The hologram reconstructions of the low viscosity liquid (Fig. 4) clearly show the streamwise evolution of primary breakup and surface wave structure. Near the jet exit, the density of ligaments leaving the surface is relatively large with distances between ligaments comparable to the wavelength of disturbances along the surface. The flow then evolves to longer wavelength disturbances along the surface with ligament sizes remaining similar to those at the jet exit but with a reduced density of ligaments leaving the surface. The near injector region suggests behavior somewhat like the turbulent breakup mechanism observed for fully-developed turbulent pipe flow at the jet exit, where liquid element sizes near the surface are comparable to the integral scale of the liquid turbulence.[3] In the present case, the comparable vortical region of the liquid would be the boundary layer thickness at the jet exit. Farther downstream, however, the disturbances of the liquid surface are more on the scale of the jet exit diameter and may be the result of helical instability of the jet along the lines of the observations of Hoyt and Taylor.[23] In this region, ligament diameters are significantly smaller than the wavelength of the surface waves, suggesting that they are due to the stripping action of the gas flow over the tips of the largest surface waves.

The hologram reconstructions for the viscous liquid (Fig. 5) are qualitatively similar to the low viscosity liquid. Near the jet exit, surface wavelengths are relatively short and the ligaments are dense and have comparable dimensions. Farther downstream, surface wavelengths become longer, comparable to the jet exit diameter, with generally smaller ligament dimensions. In this case, however, the ligaments become very long which causes the streamer-like behavior seen in the flash photographs of Fig. 3. This suggests somewhat thicker regions of liquid vorticity both near the jet exit due to boundary layers along the injector passage walls as well as along the surface of waves farther downstream. This behavior is consistent with larger thicknesses of vortical regions near the liquid surface as the liquid viscosity increases for comparable relative velocities across the mixing layer.

Drop Size Distributions

Ruff et al.[3] studied drop size distributions both along the liquid surface after primary breakup, and across the mixing layer presumably after secondary breakup. These measurements were carried out for both slug flow and fully-developed turbulent pipe flow at the jet exit — the latter condition yielding a turbulent primary breakup mechanism whose properties were correlated with liquid turbulence properties rather than potential aerodynamic effects. Nevertheless, drop size distributions for all these conditions were represented reasonably well by a universal root normal distribution proposed by Simmons[27] based on extensive observations in the dilute region of a variety of sprays. Since this assessment was limited to a single jet exit diameter and relative velocity for water injection in air, however, it was of interest to extend the evaluation to the broader range of primary breakup conditions of the present tests.

Drop size distributions measured after primary breakup during the present tests are plotted in Fig. 6. Results are shown for all liquids and relative velocities used, plotted in terms of the universal root normal distribution of Simmons.[27] The results involve a variety of distances from the jet exit but streamwise distance did not affect the nature of the distribution and is not indicated in order to reduce cluttering of the plots. The root normal distribution has two parameters, one of which can be taken to be the SMD while the other is the MMD/SMD ratio.

Simmons[27] recommends MMD/SMD = 1.2; therefore, root normal distributions in this range are also shown on the plot.

Similar to the findings of Ruff et al.[3] the root normal distribution with MMD/SMD = 1.2 yields an excellent correlation of the present measurements, except for a few outlying points. Firmly establishing drop size distributions requires sizing a large number of drops,[5,6] which is difficult for primary breakup because the drops are generally large and not very numerous. Thus, the outlying points seen at larger diameters in Fig. 6 are primarily due to insufficient numbers of drops in the distributions for some test conditions. Taking all the results as a whole, however, it was found that MMD/SMD = 1.18 with a 95 percent confidence interval of 1.14-1.22 so that Simmons' recommended value is within the range of the present measurements. This is very helpful because the entire drop size distribution can be related to the SMD in a simple manner. Thus, the following results concerning drop sizes after primary breakup will be discussed in terms of SMD.

SMD of Primary Breakup

In view of the effects of distance from the jet exit on flash photography and hologram visualizations, the first primary breakup property that was studied quantitatively was the variation of SMD with distance from the jet exit. Results for slug flow jet exit conditions from both Ruff et al.[3] and the present tests are illustrated in Fig. 7. Overall, these results include all the test liquids, grouped into several jet exit velocities.

It was found that SMD tended to increase with increasing distance from the jet exit and then approached a regime where the rate of increase was relatively slow. This latter region will be termed the fully-developed primary breakup regime in the following. Approach to fully-developed conditions was slower for the more viscous liquids, which also had more extended regions of high surface density ligament formation near the jet exit, see Figs. 4 and 5. Thus, Fig. 7 involves plots of SMD normalized by the fully-developed value, SMD_{FD}, as a function of the Reynolds number based on distance from the jet exit and liquid properties, Re_{fx}.

Results illustrated in Fig. 7 show a progressive increase of SMD with Re_{fx}, as discussed earlier. The data is relatively limited,however, fully-developed primary breakup conditions are reached for Re_{fx} on the order of 10^6. This corresponds to conditions where boundary layers typically undergo transition to turbulent flow.[28] However, the appropriate relative velocity and transition conditions for boundary layers along free surfaces and walls are not the same so that more study is needed to determine the relationship between the fully-developed primary breakup regime and turbulence in the liquid. For low viscosity materials, like water and n-heptane, fully-developed conditions are reached relatively close to the jet exit. However, for the most viscous glycerol solutions, virtually the entire region where observations are made ($x/d \leq 50$) was in the development regime. This behavior suggests a close relationship between the development of vorticity in the liquid and processes leading to primary breakup, which is consistent with the strong effect of the degree of initial flow development on mixing rates.[1,4] Certainly a uniform liquid flow region is not expected to yield conditions required to eject liquid as ligaments from a liquid surface. Instead, a region of vorticity near the surface, having a thickness controlled by boundary layer growth rates, is a better setting for ligament formation, with the thickness of this layer tending to control ligament size. Thus, increases of SMD with increasing Re_{fx} seem quite plausible.

A second feature observed in Fig. 7 is that SMD still varies somewhat in the fully-developed primary breakup regime. Two effects could be responsible for this behavior: reduced relative velocities near the liquid surface and increased wavelengths of surface waves as distance from the jet exit increases. First of all, measurements of mean velocity distributions within the multiphase mixing layer show progressively increasing gas velocities along the liquid surface with increasing distance from the jet exit.[2,3] Naturally, the resulting reduced relative velocities in the vicinity of the liquid surface would tend to increase drop sizes after primary breakup, if not eventually ending primary breakup by aerodynamic surface breakup mechanisms entirely. The second effect relates to the wavelength of liquid surface disturbances which were observed to increase with increasing distance from the jet exit during the present study. Hoyt and Taylor[23] also observe a slow but progressive increase of the wavelength of surface disturbances with increasing distance from the jet exit of liquid jets in gases for similar helical type surface waves. In this case, longer wavelengths would be expected to yield larger drop sizes after primary breakup by any of the mechanisms advanced thus far.[13-18]

In view of these observations, the transition from near injector to the fully-developed primary breakup regime may largely represent the end of breakup conditions affected by the presence of boundary layers along the passage walls at the jet exit. Thus, further consideration of primary breakup will be limited to the fully-developed regime to avoid uncertainties about affects of the degree of flow development at the jet exit, which are likely to be apparatus-dependent.

Fully-Developed Primary Breakup

A correlation of SMD after primary breakup in the fully-developed regime was sought based on the existing theoretical correlations of Taylor,[14] Levich,[15] Mayer[17] and Adelberg.[18] All these approaches yield We_{gSMD} as a function of Ta after primary breakup; therefore, a correlation of present measurements was sought as a function of these variables. The present measurements, those of Ruff et al.,[2,3] and the theoretical correlations are plotted in this manner in Fig. 8. The Taylor[14] and Levich[15] correlations are identical at small Ta, yielding Eq. (1), and have been fitted to the measurement of Ruff et al.[2,3] in that regime for the purposes of illustration. The limit of primary drop breakup proposed by Levich[15] has been illustrated at Ta = 1, although only this order of magnitude was proposed. The correlations of Mayer[17] and Adelberg[18] follow Eq. (2), with appropriate values of C_B. The measurements illustrated in Fig. 8 are limited to the fully-developed region.

Clearly, none of the theoretical expressions illustrated in Fig. 8 provide a successful correlation of the measurements. In particular, for a given liquid in air, Ta varies primarily with variations of $\bar{u}$ and the theoretical expressions do not yield the correct velocity dependence of SMD after primary breakup. For example, SMD ~ $\bar{u}^{-2}$ and $\bar{u}^{-4/3}$ for the aerodynamic and sheltered wave growth theories, while the measurements generally yield SMD ~ $\bar{u}^{-0.8}$. This difference has serious ramifications concerning the relative importance of secondary breakup and collisions in dense sprays and multiphase mixing layers. For example, Reitz and Bracco[16] estimate very small drop sizes after primary breakup by applying the aerodynamic breakup theory of Taylor[14] to the test conditions used by Hiroyasu et al.[29] The result implied that collisions within the dense spray region must be important in order to obtain drop sizes that were actually measured in the dilute portions of the spray. In contrast, the relatively low velocity dependence of the present measurements would imply significant effects of secondary breakup in the same flow. Other evidence to be

discussed later suggests that this behavior is general so that the change in sensitivity of primary breakup to changes in velocity implies that dense sprays and multiphase mixing layers are more likely to be dominated by secondary breakup than collisions, the conventional view of liquid breakup,[5] unless impinging liquid streams are considered.

Another difficulty with the correlations illustrated in Fig. 8 is that they do not accommodate effects of changing liquid properties. In particular, progressively increasing the liquid viscosity, by adding glycerin to water, causes nearly parallel shifts of the We_{gSMD} plots to higher values of Ta, but still having the same velocity dependence.

An alternative view of primary breakup yielded a more successful correlation of present measurements. The general nature of the approach is illustrated in Fig. 9 where ligament formation from a surface wave is illustrated. The reference frame taken in the figure is with respect to the wave, assuming that the relative velocity of the liquid and wave velocity are roughly the same. Then the relative motion causes a boundary layer to develop on the windward side of the wave and it is implied that drop sizes after primary breakup are comparable to the thickness of the boundary layer as it reaches the tip of the wave, i.e., that liquid is stripped from the tip of the wave, controlling its growth. This is plausible because the liquid in the bulk of the slug flow has no vorticity and cannot be deflected so that it leaves the liquid phase as a ligament. For present test conditions, wavelengths of disturbances along the surface in the fully-developed primary breakup regime were comparable to the initial jet diameter, and were probably helical waves as noted earlier. Then assuming that the SM D after primary breakup is proportional to the thickness of the surface boundary layer, that the distance that the boundary layer grows is proportional to the jet exit diameter, that the relative velocity of the layer scales as $\bar{u}_o$, and that the surface boundary layer is laminar, there results

$$SMD/d = C_B''/(\rho_f \bar{u}_o d/\mu_f)^{1/2} \qquad (3)$$

where C_B'' is an empirical constant involving the various proportionality factors. It is convenient to rearrange Eq. (3) so that We_{gSMD} is introduced because this simplifies comparison with the earlier theoretical correlations and the evaluation of secondary breakup effects. Completing this rearrangement yields:

$$We_{gSMD} = C_B'' We_{gd} / Re_{fd}^{1/2} \qquad (4)$$

Present measurements in the fully-developed primary breakup regime are plotted in terms of the variables of Eq. (4) in Fig. 10. The correlation of the data for all liquids, the full range of velocities and jet diameters of 5.0 and 9.5 mm is seen to be remarkably good. The slope of the correlation in terms of $We_{gd}/Re_{fd}^{1/2}$ is not unity as suggested by Eq. (4), however, and can be represented better by the following empirical fit which is shown on the plot:

$$We_{gSMD} = 16(We_{gd} / Re_{fd}^{1/2})^{0.82} \qquad (5)$$

The standard deviations of the coefficient and power in Eq. (5) are 6 and 4 percent, respectively, with the correlation coefficient of the fit being 0.96. The reduction of the exponent of $We_{gd}/Re_{fd}^{1/2}$ from unity in Eq. (4) to 0.82 in Eq. (5) is statistically significant but is not large in view of the qualitative nature of the development of the correlation. Equation (5) implies that SMD ~ $\bar{u}_o^{-0.77}$ which is roughly the velocity dependence observed for each liquid.

The reasonably good performance of Eqs. (4) and (5) suggests that wave growth properties determine the dimensions of surface waves but that boundary layer growth along the windward side of the wave controls drop dimensions after primary breakup. This picture is consistent with present observations that drop sizes after primary breakup were significantly smaller than surface wavelengths in the fully-developed regime because boundary layer thicknesses are generally much smaller than their length of development. This behavior is analogous to stripping-type secondary breakup of drops, where liquid boundary layers developed on the windward side of the drop, and ejecting into the gas phase at the drop periphery, have provided successful correlations of drop breakup times.[30] The importance of liquid vorticity for primary breakup is also consistent with differences observed between primary breakup near the jet exit and the fully-developed region, as well as differences between primary breakup for nonturbulent slug flow and fully-developed turbulent pipe flow at the jet exit, discussed earlier.

It is also of interest to consider the potential for secondary breakup based on the results of Fig. 10 and the universal root normal size distribution of Simmons.[27] First of all, it is generally agreed that drops are unstable to secondary breakup when their Weber number, We_{gp}, exceeds a critical value, as follows:[3,9]

$$We_{gp} = \rho_g d_p \bar{u}_o^2 / \sigma \geq 6.5 \qquad (6)$$

where Eq. (6) has been written assuming that the relative velocity of large drops subject to secondary breakup is equal to the relative velocity of the mixing layer, based on the results of Ruff et al.[2,3] Now the universal root normal distribution implies that drop sizes within three standard deviations of the mean have the diameter range $0.098 \leq d_p/SMD \leq 3.5$, and contain 99.7 percent of the spray mass. This information, combined with Eq. (6), means that We_{gSMD} = 1.8 and 66 define limiting conditions where virtually no drops or all drops undergo secondary breakup.

The limits of secondary breakup are shown in Fig. 10 along with the primary breakup correlation. Noting that it is difficult to remain in the atomization breakup regime for values of $We_{gd}/Re_{fd}^{1/2}$ much lower than the present test range, it is evident that most sprays involve significant levels of secondary breakup. Additionally, as jet velocities increase, a progressively larger fraction of the drops undergo secondary breakup. Thus, at high relative velocities, approaching conditions where the locally-homogeneous flow approximation is appropriate,[3,11] secondary breakup becomes a dominant mechanism within multiphase mixing layers.

Another effect of secondary breakup is that it tends to make We_{gSMD} more nearly constant as relative velocities change than is the case for primary breakup, correlated by Eq. (5). This helps explain the durability of primary breakup correlations like Eqs. (1) and (2) with their strong effect of relative velocity on the SMD, i.e., any contamination of the measurements by secondary breakup helps support the trends of these relationships. Since past measurements of drop sizes were carried out after the sprays became dilute, it is probable that they involved significant levels of secondary breakup. Additionally, the results of secondary breakup do not depend on the jet diameter, which also helps explain the weak, or absent, jet diameter effects seen in early correlations of primary breakup.[14-18] Finally, present measurements in the fully-developed primary breakup regime were obtained at some distance from the jet exit, providing an opportunity to convect smaller drops from primary breakup near the jet exit, as well as drops having undergone secondary breakup, into the region of the measurements. This could explain the smaller power of

$We_{gd}/Re_{fd}^{1/2}$ seen in the empirical correlation of the data, Eq. (5), than expected from Eq. (4).

Conclusions

Primary breakup within the multiphase mixing layer of the near-injector region of large-scale pressure-atomized sprays was studied, considering nonturbulent slug flow at the jet exit. The major conclusions of the study are as follows:

1. Drop size distributions after primary breakup in the mixing layer approximate Simmons' universal root normal distribution with MMD/SMD = 1.2, and can be characterized by a single parameter, e.g., the SMD.

2. The SMD after primary breakup tended to increase with increasing distance from the jet exit and then approach nearly constant values in a fully-developed primary breakup regime for Re_{fx} greater than roughly 10^6. This transition process and SMD near the injector, however, are probably apparatus-dependent because liquid vorticity tends to dominate processes of primary breakup due to the large liquid/gas density ratios of sprays.

3. Existing correlations of SMD after primary breakup based on unstable wave growth — due to Taylor,[14] Levich,[15] Mayer[17] and Adelberg[18] — were ineffective for correlating the present measurements. The main deficiencies were substantial overestimation of the rate of reduction of drop sizes with increasing relative velocities, and an inability to correctly treat effects of changes of liquid viscosity.

4. A reasonably good correlation of SMD in the fully-developed primary breakup regime — for various liquids, injector diameters and relative velocities — was achieved using Eq. (5). This expression was based on stripping-type breakup due to boundary layer growth within the liquid along the windward side of surface waves — somewhat analogous to stripping-type secondary breakup of drops.

5. The SMD and drop size distributions after primary breakup imply that most drops are subject to secondary breakup — more so as the parameter $We_{gd}/Re_{fd}^{1/2}$ increases. This means that secondary breakup, rather than collisions, is a major mechanism within multiphase mixing layers unless the flow involves impinging liquid jets.

Present results were limited to a small range of liquid/gas density ratios and particular slug flow injector designs: effects of density ratio and initial liquid vorticity conditions merit additional study as important variables affecting primary breakup properties. Furthermore, primary breakup near the end of the multiphase mixing layer should differ from present observations in the fully-developed primary breakup regime, due to the evolution of gas phase velocity distributions and instability (flapping) of the liquid core; therefore, primary breakup in this region deserves attention as well.

Acknowledgements

This research was supported by ONR Grant No. N00014-89-J-1199 with G. D. Roy serving as Scientific Officer. Initial development of the test apparatus and instrumentation was sponsored by the Air Force Office of Scientific Research, under Grant No. AFOSR-85-0244, with J. N. Tishkoff serving as Program Manager. The U.S. Government is authorized to reproduce and distribute copies of this report for governmental purposes notwithstanding any copyright notation thereon.

References

[1]Ruff, G.A., Sagar, A.D. and Faeth, G.M., "Structure of the Near-Injector Region of Pressure-Atomized Sprays," AIAA J, Vol. 27, July 1987, pp. 549-559.

[2]Ruff, G.A., Bernal, L.P. and Faeth, G.M., "Structure of the Near-Injector Region of Non - Evaporating Pressure-Atomized Sprays," J. Prop. Power, 1990, in press.

[3]Ruff, G.A., Wu, P.-K., Bernal, L.P. and Faeth, G.M., "Continuous and Dispersed-Phase Structure of Dense Nonevaporating Pressure-Atomized Sprays," J. Prop. Power, submitted.

[4]Tseng, L.-K., Ruff, G.A. and Faeth, G.M., "Effects of Ambient Gas Density on the Structure of Pressure-Atomized Sprays," AIAA Paper No. 91-0690, 1991.

[5]Giffen, E. and Muraszew, A., The Atomization of Liquid Fuels, John Wiley & Sons, New York, 1953.

[6]Lefebvre, A.H., "Airblast Atomization," Prog. Energy Combust. Sci., Vol. 6, 1980, pp. 223-246.

[7]Harrje, D.T. and Reardon, F.H., Liquid Rocket Combustion Instability, NASA SP-194, 1972, pp. 49-55.

[8]McCarthy, M.J. and Malloy, N.A., "Review of Stability of Liquid Jets and the Influence of Nozzle Design," Chem. Engr. J., Vol. 7, 1974, pp. 1-20.

[9]Clift, R., Grace, J.R. and Weber, M.E., Bubbles, Drops and Particles, Academic Press, New York, 1978, p. 346.

[10]Faeth, G.M., "Mixing, Transport and Combustion in Sprays," Prog. Energ Combust Sci., Vol. 13, 1987, pp. 298-345.

[11]Faeth, G.M., "Structure and Atomization Properties of Dense Turbulent Sprays," Twenty-Third Symposium (International) on Combustion, The Combustion Institute, Pittsburgh, 1990, in press.

[12]Miesse, C.C., "Correlation of Experimental Data on Disintegration of Liquid Jets," Ind. Engr. Chem., Vol. 47, Sep. 1955, pp. 1690-1697.

[13]Ranz, W.E., "Some Experiments on Orifice Sprays," Canadian Journal of Chemical Engineering, Vol. 36, Aug. 1958, pp. 175-181.

[14]Taylor, G.I., "Generation of Ripples by Wind Blowing Over a Viscous Liquid," The Scientific Papers of Sir Geoffrey Ingram Taylor, Vol. III, edited by G.K. Batchelor, Cambridge Univ. Press, Cambridge, England, 1963, pp. 244-254.

[15]Levich, V. G., Physicochemical Hydrodynamics, Prentice-Hall, Inc., Englewood Cliffs, NJ, 1962, pp. 639-646.

[16]Reitz, R.D. and Bracco, F.V., "Mechanism of Atomization of a Liquid Jet," Phys. Fluids, Vol. 25, Oct. 1982, pp. 1730-1742.

Table 1 Summary of Test Conditions[a]

Liquid	ρ_f (kg/m^3)	$\mu_f \times 10^4$ (kg/ms)	$\sigma \times 10^2$ (N/m)	d (mm)	$\bar{u}_0$ (m/s)	$Re_{fd} \times 10^{-4}$ (-)	We_{gd} (-)	$Oh \times 10^3$ (-)
water[b]	997	8.94	7.08	9.5	56.4	60	499	1.09
water	997	8.94	7.08	5.0	28.1-133.8	16-75	94-1480	1.50
n-heptane	683	3.97	2.00	5.0	16.5-72.1	14-62	80-1520	1.52
glycerol 12%	1044	15.92	6.43	5.0	30.4-89.2	10-29	84-724	2.75
glycerol 42%	1101	34.66	6.30	5.0	29.3-90.6	4.7-14	80-762	5.89
glycerol 63%	1158	108.30	6.20	5.0	31.2-90.2	1.7-4.8	92-768	18.1

[a]Pressure-atomized injection vertically downward in still air at 98.8 kPa and 238 ± 3K with nonturbulent jet exit conditions.

[b]Results from the steady flow arrangement of Ruff et al.[2,3]

[17]Mayer, E., "Theory of Liquid Atomization in High Velocity Gas Streams," ARS J, Vol. 31, 1961, pp. 1783-1785.

[18]Adelberg, M, "Mean Drop Size Resulting from the Injection of a Liquid Jet into a High-Speed Gas Stream," AIAA J, Vol. 6, 1968, pp. 1143-1147.

[19]Jeffreys, H., "On the Formation of Water Waves by Wind," Proc. Royal Soc. London, Vol. A110, 1926, pp. 241-247.

[20]Weiss, M.A. and Worsham, C.H., "Atomization in High Velocity Airstreams," ARS J, Vol. 29, April 1959, pp. 252-258.

[21]Phinney, R.E., "The Breakup of a Turbulent Jet in a Gaseous Atmosphere," J. Fluid Mech., Vol. 6, Oct. 1973, pp. 689-701.

[22]Hoyt, J.W. and Taylor, J.J., "Turbulence Structure in a Water Jet Discharging in Air," Phys. Fluids, Vol. 20, Pt. II, Oct. 1977, pp. S253-S257.

[23]Hoyt, J.W. and Taylor, J.J., "Waves on Water Jets," J. Fluid Mech., Vol. 83, 1977, pp. 119-127.

[24]Hoyt, J.W. and Taylor, J.J., "Effect of Nozzle Boundary Layer on Water Jets Discharging in Air," Jets and Cavities (J.H. Kim, O. Furuya and B.R. Parkin, ed.) ASME-FED, Vol. 31, ASME, New York, 1985, pp. 93-100.

[25]Smith, R.N. and Wang, C.-T., "Contracting Cones Giving Uniform Throat Speeds," J. Aero. Sci., Vol. 11, Oct. 1944, pp. 356-360.

[26]Ramjee, V. and Hussain, A.K.M.F., "Influence of the Axisymmetric Contraction Ratio on Free-Stream Turbulence," J. Fluids Engrg., Vol. 198, Sep. 1976, pp. 506-515.

[27]Simmons, H.C., "The Correlation of Drop Size Distributions in Fuel Nozzle Sprays," J. Engrg. for Power, Vol. 99, 1977, pp. 309-319.

[28]Schlichting, W., Boundary Layer Theory, 7th ed., McGraw-Hill, New York, 1979, p. 599.

[29]Hiroyasu, H., Shimizu, M., and Arai, M., "The Breakup of a High Speed Jet in a High Pressure Gaseous Environment," Univ. Of Wisconsin, Madison, ICLASS-82, 1982.

[30]Ranger, A.A. and Nicholls, J.A., "Aerodynamic Shattering of Liquid Drops," AIAA J, Vol. 7, Feb. 1969, pp. 285-290.

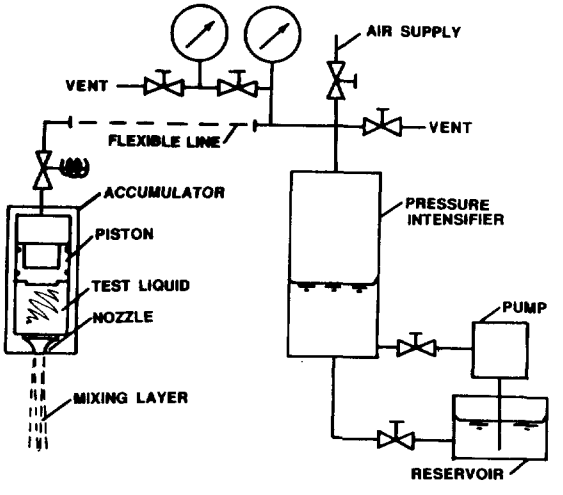

Fig. 1 Sketch of high-speed multiphase mixing layer apparatus.

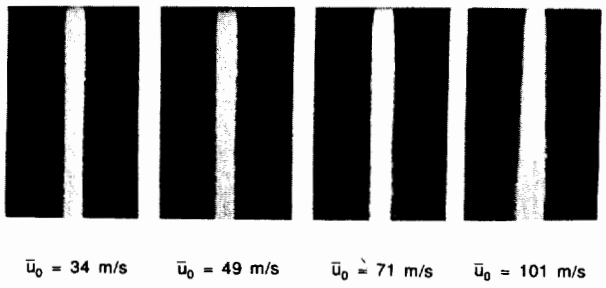

Fig. 2 Flash photographs of low viscosity (water) jets at various jet exit velocities.

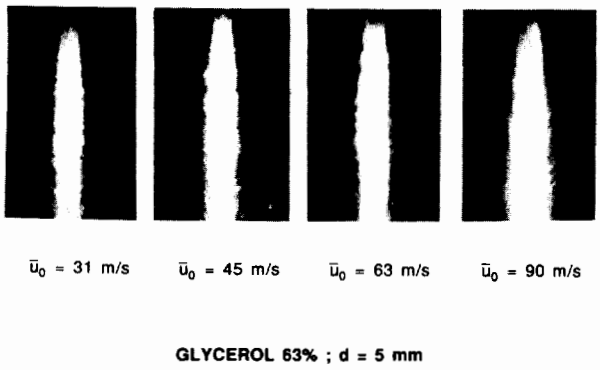

Fig. 3 Flash photographs of high viscosity (glycerol, 63percent) jets at various jet exit velocities.

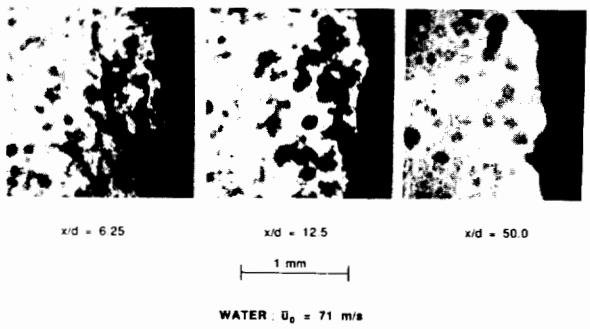

Fig. 4 Hologram reconstructions of low viscosity (water) jets at various distances from jet exit.

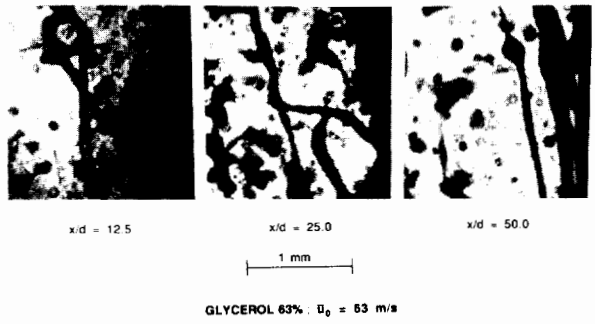

Fig. 5 Hologram reconstructions of high viscosity (glycerol, 63 percent) jets at various distances from jet exit.

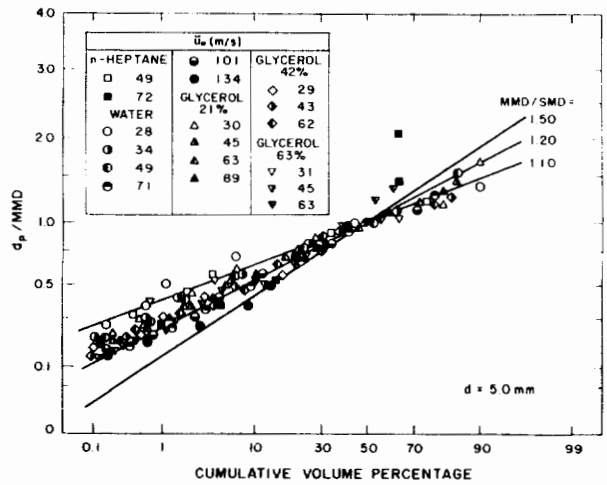

Fig. 6 Drop size distributions after primary breakup.

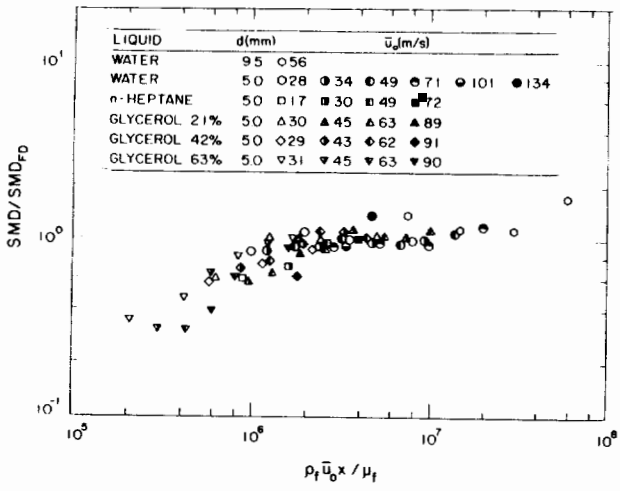

Fig. 7 Streamwise variation of SMD after primary breakup.

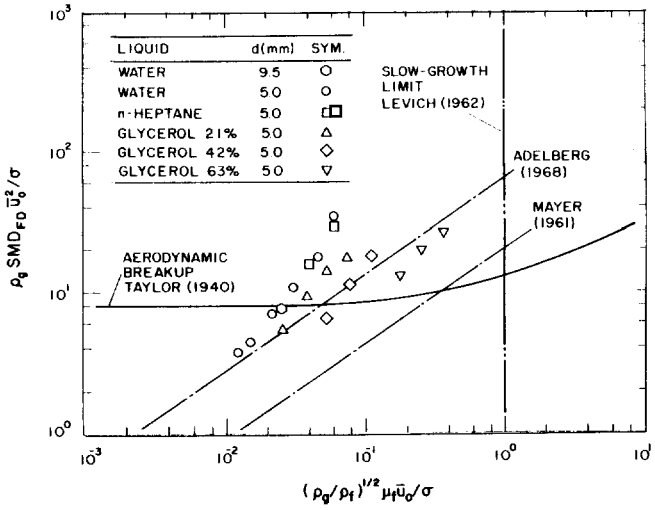

Fig. 8 Correlation of SMD after primary breakup in the fully-developed region according to existing theories.

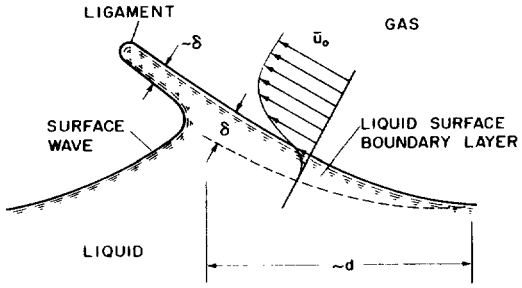

Fig. 9 Sketch of the shear-type primary breakup mechanism.

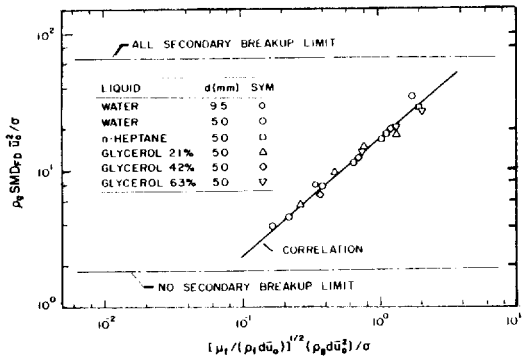

Fig. 10 Correlation of SMD after primary breakup in the fully-developed region.